THE JOURNAL OF BIOLOGICAL CHEMISTRY VOL. 290, NO. 33, pp. 20427–20437, August 14, 2015
Published in the U.S.A.

Role of Deacetylase Activity of *N*-Deacetylase/*N*-Sulfotransferase 1 in Forming *N*-Sulfated Domain in Heparan Sulfate*

Received for publication, May 10, 2015, and in revised form, June 16, 2015 Published, JBC Papers in Press, June 24, 2015, DOI 10.1074/jbc.M115.664409

Wenfang Dou[‡§1], **Yongmei Xu**[‡], **Vijayakanth Pagadala**[‡], **Lars C. Pedersen**[¶], **and Jian Liu**[‡2]

From the [‡]*Division of Chemical Biology and Medicinal Chemistry, Eshelman School of Pharmacy, University of North Carolina, Chapel Hill, North Carolina 27599, the* [§]*Laboratory of Pharmaceutical Engineering, School of Pharmaceutical Sciences, Jiangnan University, Wuxi 214122, China, and the* [¶]*Genome Integrity and Structural Biology Laboratory, NIEHS, National Institutes of Health, Research Triangle Park, North Carolina 27709*

Background: *N*-Deacetylase/*N*-Sulfotransferase is a bifunctional enzyme in the heparan sulfate biosynthetic pathway.
Results: *N*-Deacetylase and *N*-sulfotransferase domains display cooperative effects as a bifunctional enzyme; individually expressed *N*-deacetylase and *N*-sulfotransferase domains do not exhibit the same level of cooperativity.
Conclusion: The bifunctionality of *N*-deacetylase/*N*-sulfotransferase is required to form N-S domain in heparan sulfate.
Significance: This work uncovers the process by which NDST-1 constructs functional heparan sulfate.

Heparan sulfate (HS) is a highly sulfated polysaccharide that plays important physiological roles. The biosynthesis of HS involves a series of enzymes, including glycosyltransferases (or HS polymerase), epimerase, and sulfotransferases. *N*-Deacetylase/*N*-Sulfotransferase isoform 1 (NDST-1) is a critical enzyme in this pathway. NDST-1, a bifunctional enzyme, displays *N*-deacetylase and *N*-sulfotransferase activities to convert an *N*-acetylated glucosamine residue to an *N*-sulfo glucosamine residue. Here, we report the cooperative effects between *N*-deacetylase and *N*-sulfotransferase activities. Using baculovirus expression in insect cells, we obtained three recombinant proteins: full-length NDST-1 and the individual *N*-deacetylase and *N*-sulfotransferase domains. Structurally defined oligosaccharide substrates were synthesized to test the substrate specificities of the enzymes. We discovered that *N*-deacetylation is the limiting step and that interplay between the *N*-sulfotransferase and *N*-deacetylase accelerates the reaction. Furthermore, combining the individually expressed *N*-deacetylase and *N*-sulfotransferase domains produced different sulfation patterns when compared with that made by the NDST-1 enzyme. Our data demonstrate the essential role of domain cooperation within NDST-1 in producing HS with specific domain structures.

Heparan sulfate (HS)[3] is a highly sulfated linear polysaccharide ubiquitously present on the cell surface and in the extracellular matrix. HS has a wide range of biological functions, including embryonic development, inflammatory response, response to viral and bacterial infection, and regulation of blood coagulation (1). The disaccharide repeating unit of HS consists of glucosamine or either glucuronic acid (GlcA) or iduronic acid. Both the iduronic acid (less frequently for GlcA) and glucosamine saccharides carry sulfo groups. The location of the sulfo groups and the placement of iduronic acid play a crucial role in determining the functions of HS (2). Specialized enzymes such as HS polymerase, C_5-epimerase, and sulfotransferases participate in synthesizing HS (Fig. 1*A*). HS polymerase is responsible for producing the polysaccharide backbone with a repeating unit of -GlcA-GlcNAc-. The backbone is then modified by *N*-deacetylase/*N*-sulfotransferase (NDST), C_5-epimerase, 2-*O*-sulfotransferase, 6-*O*-sulfotransferase, and 3-*O*-sulfotransferase. The substrate specificities of the biosynthetic enzymes ultimately dictate the structures of HS (3). Understanding the biosynthetic mechanism of HS is critically important for delineating the structure/function relationship of HS as well as for improving a chemoenzymatic approach to synthesize HS-based therapeutics (4, 5).

NDST is a bifunctional enzyme that converts GlcNAc residues to *N*-sulfo glucosamine (GlcNS) residues. The *N*-deacetylase domain removes the acetyl group from GlcNAc to form *N*-unsubstituted glucosamine ($GlcNH_2$), whereas the *N*-sulfotransferase domain transfers a sulfo group to the $GlcNH_2$ residues to form GlcNS (Fig. 1*B*). The NDST modification step is essential for the biosynthesis of HS as other HS biosynthetic enzymes, such as C_5-epimerase (6, 7), 2-*O*-sulfotransferase (8, 9), and 3-*O*-sulfotransferase (10), all require the presence of GlcNS residues to complete their modifications (Fig. 1*A*). A total of four NDST isoforms are present in the human genome (11, 12). Among these isoforms, NDST-1 is the most widely expressed and has profound physiological implications. The NDST-1 knock-out mice displayed respiratory distress, causing

* This work was supported in part by National Institutes of Health Grants GM102137 and HL094463 and by the Division of Intramural Research of the NIEHS, National Institutes of Health Research Project number ZIA ES102645 (to L. C. P.). The authors declare that they have no conflicts of interest with the contents of this article.
[1] Partially supported by a fellowship from the China Scholarship Council.
[2] To whom correspondence should be addressed: Rm. 1044, Genetic Medicine Bldg., 120 Mason Farm Rd., University of North Carolina, Chapel Hill, NC 27599. Tel.: 919-843-6511; E-mail: jian_liu@unc.edu.
[3] The abbreviations used are: HS, heparan sulfate; NDST, *N*-deacetylase/*N*-sulfotransferase; NDase, *N*-deacetylase; NST, *N*-sulfotransferase; GlcA, glucuronic acid; GlcNS, *N*-sulfo glucosamine; PAPS, 3′-phosphoadenosine 5′-phosphosulfate; pNP, *p*-nitrophenyl; GlcA-pNP, *p*-nitrophenyl glucuronide; GlcNTFA, trifluoroacetylglucosamine; PAMN, polyamine; OST, *O*-sulfotransferase; ESI, electrospray ionization.

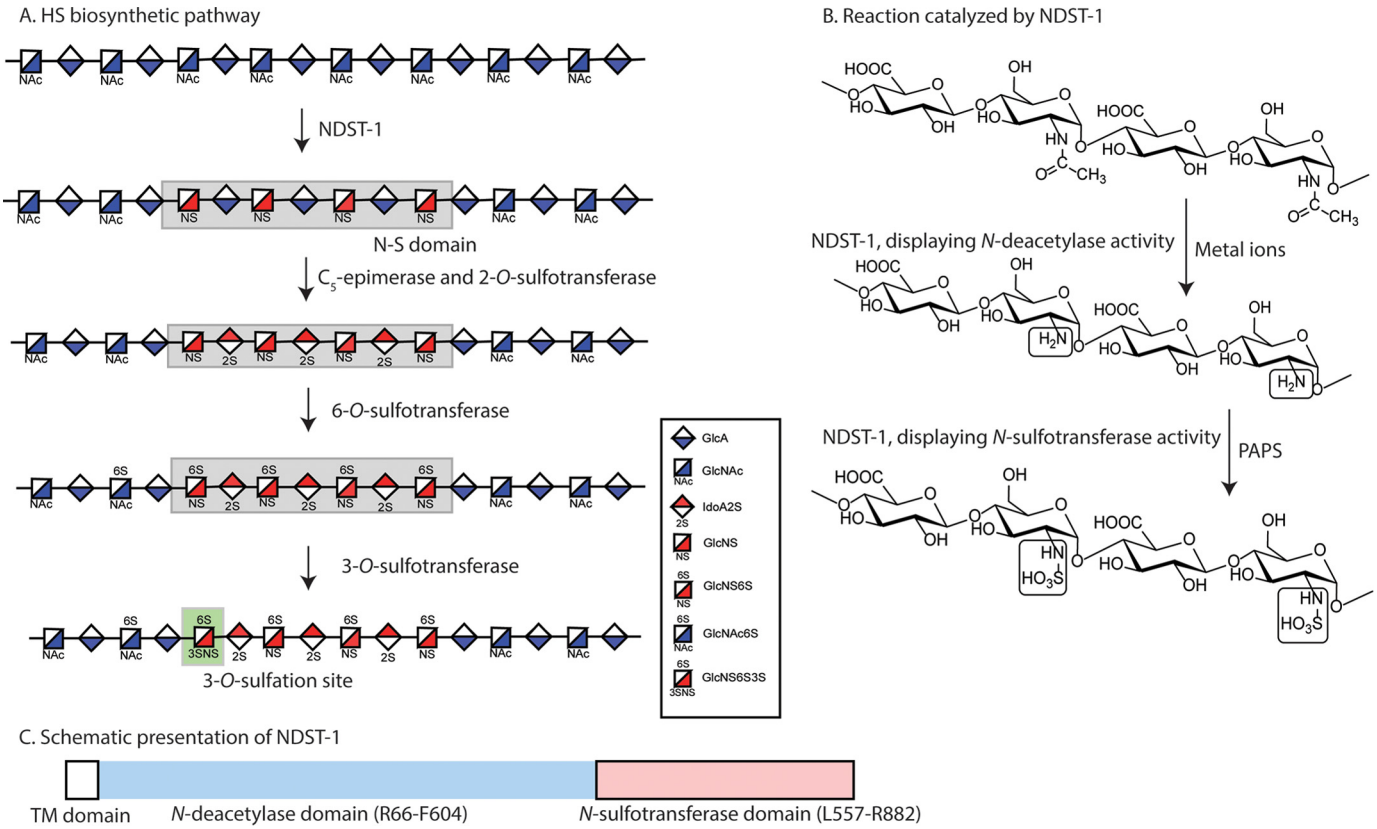

FIGURE 1. **HS biosynthetic pathway and reaction catalyzed by NDST-1.** *A*, enzymatic modification steps required to produce HS. The polymerization step to form the polysaccharide backbone (-GlcA-GlcNAc-) is not shown. After NDST-1 modification, the polysaccharide undergoes C_5-epimerization and 2-*O*-sulfation followed by 6-*O*-sulfation and more limited 3-*O*-sulfation. The shorthand keys for the symbols are depicted on the *right side* of the panel. *B*, reactions catalyzed by NDST-1. Two steps are involved to convert a GlcNAc residue to a GlcNS residue. First, NDST-1 removes the acetyl group to form $GlcNH_2$, and the activity at this step is designated as *N*-deacetylase activity. Second, a sulfo group is transferred from the sulfo donor PAPS to the amino group to form GlcNS. *C*, locations of *N*-deacetylase and *N*-sulfotransferase domains in NDST-1. *TM* represents the transmembrane domain.

neonatal death (13). Conditional knock-out of NDST-1 uncovered a series of physiological and pathological roles, including lipoprotein clearance (14), development of lobuloalveolar of mammary gland (15), neutrophil trafficking (16), and inhibition of tumor angiogenesis (17). Recently, mutations in NDST-1 have been linked to autosomal recessive intellectual disability in humans, manifesting cognitive and learning impairment (18). Conversely, NDST-2 and NDST-3 knock-out mice exhibited relatively mild phenotypes (19, 20).

Structural analysis of HS isolated from natural sources indicates that the GlcNS residues are not evenly distributed along the HS chain, instead forming clusters known as N-S domains (21). Formation of the N-S domain enhances the downstream modification reactions, resulting in functional HS that displays high affinity binding to proteins (22). We previously demonstrated that NDST-1 has the ability to form the N-S domains, providing the means to synthesize biologically active HS (23). In this work, we investigate the relationship between *N*-deacetylase and *N*-sulfotransferase activities in the process of converting GlcNAc residues to GlcNS, as well as the ability to form N-S domain structures. The present study utilizes highly purified recombinant proteins and structurally defined oligosaccharide substrates to provide accurate structural analysis of the products. In addition to expressing full-length NDST-1, we successfully expressed the *N*-deacetylase and *N*-sulfotransferase domains separately, allowing us to identify cooperation between *N*-deacetylase and *N*-sulfotransferase activities. Although both individually expressed domains display their respective activities, when combined, they do not generate the product that contains N-S domains. This result demonstrates the cooperative nature of the bifunctional NDST-1 and its critical role in generating functional HS.

Experimental Procedures

Preparation of NDST-1, NDase, and NST Expression Plasmids—The clone containing the sequence for full-length human NDST-1 was purchased from Open Biosystems (Huntsville, AL). Secreted forms of recombinant proteins were prepared for this study. The primers, 5′-ATGAATTCAGTCGCCCCTAGCCGCCTCCT-3′ and 5′-TTACTCGAGCTACCTGGTGTTCTGGAGGT-3′, were used for amplifying full-length NDST-1 (Val^{62}–Arg^{882}). The primers, 5′-TATGAATTCACGCCTCCTGCCAATCAAGC-3′ and 5′-TTACTCGAGCTAGAAGCGGTCACATGTCTTC-3′, were used for amplifying the *N*-deacetylase (NDase) domain (Arg^{66}–Phe^{604}). The primers, 5′-TATGAATTCACTGCAGACTCTGCCCC-3′ and 5′-TTACTCGAGCCTGGTGTTCTGGAGGT-3′, were used for amplifying the *N*-sulfotransferase (NST) domain (Leu^{557}–Arg^{882}). The restriction sites of EcoRI and XbaI used for subcloning are underlined. The PCR reactions were performed to amplify NDST-1, NDase, and NST by heating samples to 95 °C for 5 min followed by 30 cycles of 95 °C for

30 s, 55 °C for 30 s, 70 °C for 2 min, and 70 °C for 10 min. The resulting PCR products were cloned into the pFastBac-mal-HT vector using EcoRI and XbaI sites to form NDST-1, NDase, and NST carrying a His_6 tag at the N terminus (24). All construct sequences were verified by the University of North Carolina Genome Analysis Facility. The preparation of recombinant baculovirus stocks harboring the targeted protein gene of interest was completed according to the manufacturer's instructions (Invitrogen).

Expression and Purification of NDST-1, NDase, and NST—Expression of the recombinant proteins was carried out in Sf9 cells grown in Sf-900 III SFM (Life Technologies) in 1-liter plastic shaker flasks with vented caps (200 ml of culture per flask) at 28 °C. When the cell density reached 2.0×10^6 cells ml^{-1}, recombinant virus was introduced to infect the cells. The target protein in the condition medium was harvested ~96 h after infection by centrifugation at 16,000 × g for 30 min. The resultant medium was mixed with an equal volume of 20 mM MOPS, pH 7.0 buffer, and was filtered through a Whitman glass microfiber filter (1.2 μm, Fisher) before the purification.

All three recombinant proteins were purified following a very similar protocol at 4 °C. The diluted and filtered medium was applied to a heparin-Toyopearl gel (Tosoh Bioscience) column (1.2 × 10 cm) at a flow rate of 4 ml min^{-1} and washed with buffer 1 (20 mM MOPS, 50 mM NaCl, 2% glycerol, pH 7.0). The protein was eluted with buffer 2 (20 mM MOPS, 1 M NaCl, 2% glycerol, pH 7.0). Fractions containing NDST-1, NDase, or NST were pooled and dialyzed against a buffer containing 25 mM Tris, pH 7.5, 30 mM imidazole, and 500 mM NaCl using a 14,000 molecular weight cut-off membrane (Fisher). The dialyzed samples were applied to a nickel-agarose (GE Healthcare) column (0.6 × 5.0 cm) at a flow rate of 0.5 ml min^{-1} and washed with a buffer containing 25 mM Tris, pH 7.5, 30 mM imidazole, and 500 mM NaCl followed by washing the column with the same buffer containing 64 mM imidazole until the optical density (280 nm) of the eluent reached baseline. The protein was then eluted with 300 mM imidazole in 25 mM Tris, pH 7.5, and 500 mM NaCl. The protein was stored at −80 °C for the experiments. The protein concentrations were determined by Bradford reagent (Sigma), and the purities were determined to be greater than 90% using 12% SDS-PAGE (Bio-Rad).

Determination of N-Deacetylase/N-Sulfotransferase, N-Deacetylase, and N-Sulfotransferase Activity—To measure the activity of *N*-deacetylase/*N*-sulfotransferase, heparosan (10 μg) was incubated with NDST-1 (10 ng) in a 100-μl reaction volume containing 50 mM MES, pH 7.0, 10 mm $MnCl_2$, PAPS (50 μM and 1×10^6 cpm of [^{35}S]PAPS) at 37 °C for 1 h. The reaction was stopped by adding 100 μl of a solution containing 50 mM sodium acetate, pH 5.0, 150 mM sodium chloride, 3 M urea, 1.5 mM EDTA, and 0.1% Triton X-100. The ^{35}S-labeled polysaccharide product was purified by a DEAE column. The extent of ^{35}S incorporation was determined by scintillation counting.

To measure *N*-deacetylase activity, heparosan (10 μg) was incubated with NDST-1 (10 ng) in a 100-μl reaction volume containing 50 mM MES, pH 7.0, 10 mM $MnCl_2$ at 37 °C for 1 h. The reaction was stopped by heating at 100 °C for 5 min. To the reaction mixture, 20 μg of recombinant NST expressed in *Escherichia coli* (25), unlabeled PAPS (50 μM), and [^{35}S]PAPS (1×10^6 cpm) were added, and the reaction was incubated at 37 °C for 1 h. The ^{35}S-labeled polysaccharide product was then purified and quantified using a DEAE column as described above. One unit of *N*-deacetylase activity was defined as the transfer of 1000 cpm of ^{35}S-labeled sulfo group to heparosan under this condition.

To measure *N*-sulfotransferase activity, deacetylated heparosan (10 μg) that was prepared via a chemical approach (26) was incubated with the protein (10 ng) and [^{35}S]PAPS (1×10^6 cpm) and unlabeled PAPS (50 μM) in a buffer containing 50 mM MES, pH 7.0, and 10 mM $MnCl_2$ at 37 °C for 1 h. The reaction was stopped by adding 100 μl of a solution containing 50 mM sodium acetate, pH 5.0, 150 mM sodium chloride, 3 M urea, 1.5 mM EDTA, and 0.1% Triton X-100. The ^{35}S-labeled polysaccharide product was purified by a DEAE column. One unit of *N*-sulfotransferase activity was defined as the transfer of 1000 cpm of ^{35}S-labeled sulfo group to deacetylated heparosan under this condition.

Determination of the Effects of EDTA on the Individual N-Sulfotransferase and N-Deacetylase Activities—To determine the effect of EDTA on the *N*-deacetylase activity, a range of concentrations (0.25–10 mM) of EDTA was tested in the reaction mixture containing NDST-1 and heparosan. In this experiment, Mn^{2+} (10 mM) was omitted from the reaction buffer. To measure the extent of deacetylation, recombinant *N*-sulfotransferase expressed in *E. coli* (20 μg) and [^{35}S]PAPS (25) were used to sulfate the product. The level ^{35}S incorporation correlated to the level of deacetylation in the polysaccharide product. To determine the effect of EDTA on *N*-sulfotransferase activity, 1 mM of EDTA was mixed with NDST-1, deacetylated heparosan, and [^{35}S]PAPS in the reaction buffer that did not contain Mn^{2+}.

Determination of the Effects of Metal Ions on the Full-length N-Deacetylase/N-Sulfotransferase Activity—Different metal ions (10 mM), including Ca^{2+}, Mn^{2+}, Mg^{2+}, Zn^{2+}, Co^{2+}, or Cu^{2+}, were added in the reaction mixture containing NDST-1, heparosan, and [^{35}S]PAPS. The activity was measured following the standard procedure as described above. To prepare metal-free NDST-1, purified NDST-1 protein was incubated with 1 mM EDTA and then dialyzed using a 1000 molecular weight cut-off membrane against 200 mM NaCl, 25 mM MOPS, pH 7.0 for 24 h to remove EDTA and EDTA/metal ion complex.

Preparation of 8-mer and 18-mer Substrates—8-mer and 18-mer oligosaccharide substrates were elongated from *p*-nitrophenyl glucuronide (GlcA-pNP) as reported previously (27). Briefly, GlcA-pNP (100 mg) was incubated with UDP-monosaccharide donor (UDP-GlcNAc, UDP-GlcNTFA, or UDP-GlcA) and 30 mg of PmHS2, the bacterial glycosyltransferase (heparosan synthase 2 from *Pasteurella multocida*) in 200 ml of reaction buffer containing 25 mM Tris (pH 7.2) and 10 mM $MnCl_2$. The reaction was incubated for 16 h at room temperature and analyzed by a silica-based polyamine (PAMN) HPLC column (Waters). The product was purified by a C_{18}-column (0.75 × 20 cm, Biotage) and eluted with a solution containing 70% acetonitrile and 0.1% trifluoroacetic acid. The reaction cycle was repeated seven times to attain 8-mer with a structure of GlcNAc-GlcA-GlcNTFA-GlcA-GlcNAc-GlcA-GlcNAc-GlcA-pNP. The conversion of the GlcNTFA to $GlcNH_2$ residue

was completed by incubating the 8-mer product with 0.1 M LiOH at 4 °C for 1 h. The structure of the product was confirmed by electrospray ionization mass spectrometry (ESI-MS). Approximately 180 mg of the 8-mer substrate was obtained.

The synthesis of the 18-mer substrate essentially followed the same protocol by repeating the elongation reaction 17 times. However, a different purification method was used to prepare the 18-mer substrate. Because the binding affinity of the pNP-tagged oligosaccharides to the C18-column decreases as the size of the oligosaccharide increases, a Q-Sepharose column was introduced to isolate the oligosaccharide intermediates when the sizes were larger than octasaccharide. Under this condition, the sample was loaded onto a Q-Sepharose column that was equilibrated with 25 mM Tris, pH 7.5, and 50 mM NaCl. The oligosaccharide product and intermediates were eluted from the column (1 × 30 cm) via a gradient of NaCl from 50 to 500 mM at a flow rate of 2 ml min^{-1}. The product was determined by exploiting the UV absorbance of the pNP tag at 310 nm, and the identity of the product was confirmed by ESI-MS.

Modification of the 8-mer Substrate with NDST-1 Displaying N-Deacetylase, N-Sulfotransferase, and N-Deacetylase/N-Sulfotransferase Activities—Enzyme modifications on the 8-mer substrate were performed in a similar manner as with the heparosan substrate except that 15 μg of 8-mer substrate was used in the presence of 200 ng of protein. To measure the *N*-sulfotransferase activity, 50 μM PAPS was added along with 1 mM EDTA to inhibit the deacetylase reaction. Enzyme-modified oligosaccharides were analyzed by a PAMN-HPLC column, which was eluted with a linear gradient from 0 to 1 M KH_2PO_4 over 40 min at a flow rate of 0.5 ml min^{-1}. Different peaks were collected and dialyzed prior to ESI-MS analysis.

Modification of 18-mer Substrate by NDST-1 or by the Mixture of NDase and NST—20 μg of the 18-mer substrate was incubated with NDST-1 (800 ng) or NDase/NST (650 ng for each protein) in a 200-μl buffer containing 50 mM MES buffer, pH 7.0, 10 mM $MnCl_2$, and 1 mM PAPS at 37 °C for 24 h. Enzyme-modified oligosaccharides were analyzed PAMN-HPLC. Different peaks were collected and dialyzed prior to ESI-MS analysis.

ESI-MS Analysis of Oligosaccharides—MS analysis was performed on a Thermo LCQ-Deca. The oligosaccharides were dissolved in H_2O and injected via direct infusion (50 μl min^{-1}) into the instrument. The experiments were performed by utilizing a negative ionization mode with a spray voltage of 3 KV and a capillary temperature of 120 °C. For MS/MS experiments, selection of each precursor ion was achieved using an isolation width of 3 Da, and the activation energy was 40% normalized collision energy. The MS and MS/MS data were acquired and processed using Xcalibur 1.3 software.

Nitrous Acid Depolymerization of N-[^{35}S]Sulfo-heparosan and Bio-Gel P-10 Analysis—100 μg of heparosan was incubated with NDST-1 (1 μg) or NDase/NST (1 μg of each protein) in a buffer containing 50 mM MES, pH 7.0, 10 mM $MnCl_2$, 50 μM PAPS, and [^{35}S]PAPS (5 × 10^6 cpm), at 37 °C for 24 h. The ^{35}S-labeled polysaccharide product was then purified by a DEAE column and desalted by dialysis. The resultant *N*-[^{35}S]sulfo-heparosans were deacetylated with hydrazine (Aldrich) at 95 °C and degraded with nitrous acid at pH 5.5 followed by reduction with sodium borohydride as described by Shively and Conrad (28). The resultant ^{35}S-labeled depolymerized polysaccharides were resolved on a Bio-Gel P-10 column (0.75 × 200 cm, Bio-Rad), which was equilibrated with 20 mM Tris (pH 7.5) and 1 M NaCl at a flow rate of 4 ml h^{-1}. The amount of ^{35}S radioactivity from each fraction was determined by scintillation counting.

Results

Divalent Metal Ions Are Required for N-Deacetylase Activity, but Not Required for N-Sulfotransferase Activity—NDST-1 protein has both *N*-deacetylase and *N*-sulfotransferase activities. Divalent ions, including Mn^{2+}, Mg^{2+}, and Ca^{2+}, are reportedly required for enzymatic activity (29). However, it was unclear whether the metal ions are necessary for the *N*-deacetylase activity or for the *N*-sulfotransferase activity. By choosing an appropriate polysaccharide substrate, we selectively measured the *N*-sulfotransferase activity or the *N*-deacetylase activity, respectively, as described in a previous publication (illustrated at *bottom* of Fig. 2) (30). For example, heparosan was chosen as a substrate to measure the *N*-deacetylase activity as it contains the GlcNAc residues, whereas chemically deacetylated heparosan was used to measure the activity of *N*-sulfotransferase as the substrate contains $GlcNH_2$ residues. We found no effect on the sulfotransferase activity of NDST-1 by the addition of 1 mM EDTA, a chelator for divalent ions (Fig. 2*A*). The deacetylase activity, on the other hand, was inhibited by the addition of EDTA in a dose-dependent manner (Fig. 2*B*), suggesting that divalent ions are required for *N*-deacetylase activity. The addition of different metal ions to the EDTA-treated, metal ion-free, NDST-1 protein demonstrated that divalent ions, including Mn^{2+}, Mg^{2+}, Co^{2+}, and Ca^{2+}, were able to rescue the *N*-deacetylase activity of NDST-1, whereas Zn^{2+} and Cu^{2+} were not (Fig. 2*C*). As expected, Mn^{2+}, Mg^{2+}, Co^{2+}, and Ca^{2+} also rescued the activity of *N*-deacetylase (data not shown). Further analysis indicated that Zn^{2+} and Cu^{2+} completely inhibited *N*-sulfotransferase activities at the concentration of 10 mM (data not shown). Also, the addition of Zn^{2+} or Cu^{2+} was unable to rescue the activity of *N*-deacetylase.

Previously, Riesenfeld *et al.* (31) identified the requirement of Mn^{2+} ions for the *N*-deacetylase activity, but the authors claimed that Ca^{2+} and Mg^{2+} did not activate *N*-deacetylase. Here, we demonstrate that both Ca^{2+} and Mg^{2+} clearly activate the NDST-1. The different results from the two studies can probably be attributed to the use of different substrates. Heparosan, an unmodified version of HS, was used as a substrate in our present study, whereas chemically modified HS was used in the Riesenfeld study.

The Participation of N-Sulfotransferase Accelerates N-Deacetylase Activity—The reactivity toward *N*-deacetylase and *N*-sulfotransferase activity of NDST-1 protein was selectively measured using a synthetic octasaccharide substrate (8-mer substrate). The substrate has a uniquely designed structure of GlcNAc-GlcA-$GlcNH_2$-GlcA-GlcNAc-GlcA-GlcNAc-GlcA-pNP, which can be used to test the effect of *N*-sulfotransferase and *N*-deacetylase activity as well as both activities. The 8-mer substrate contains one $GlcNH_2$ residue (at residue 3, Fig. 3*A*)

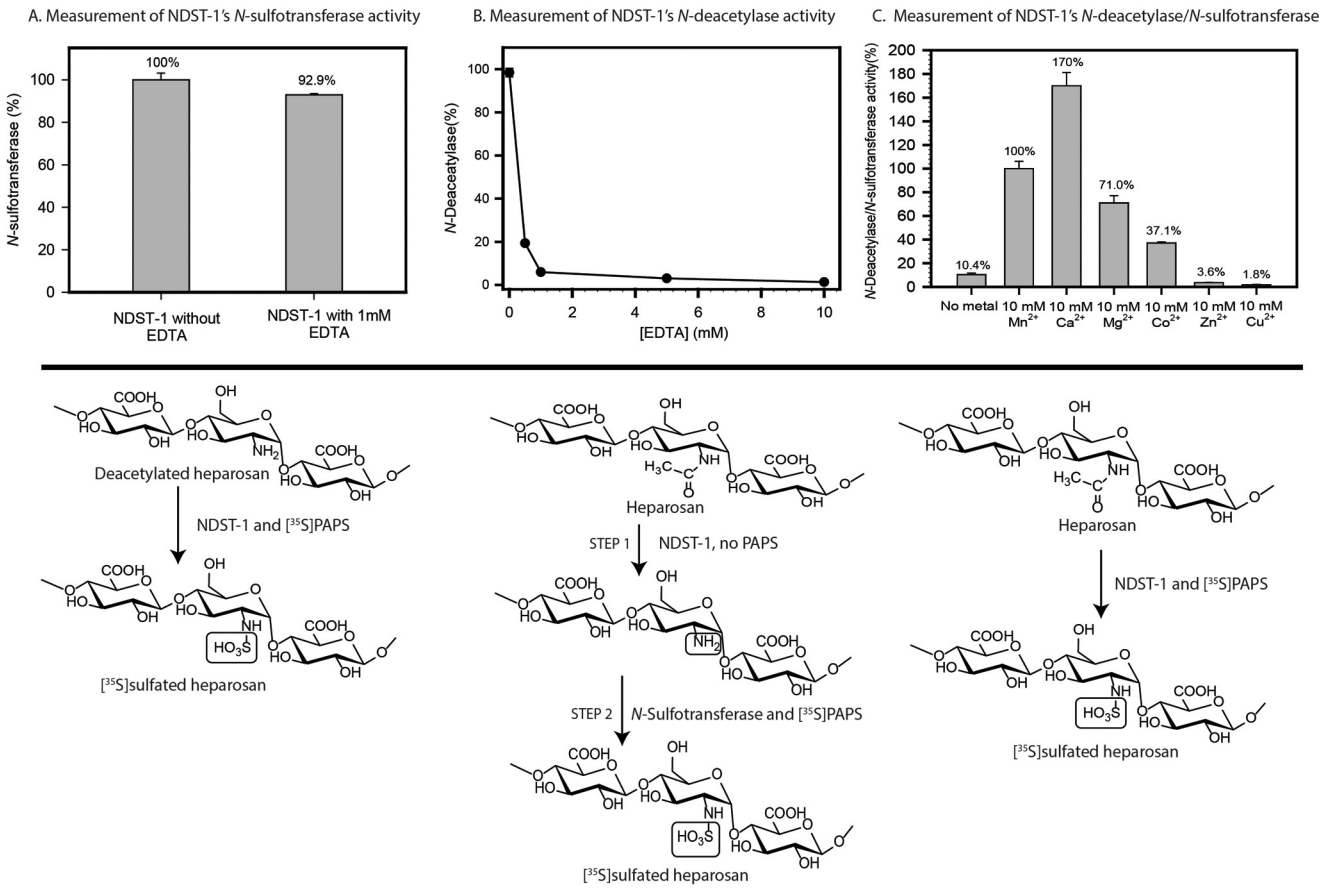

FIGURE 2. **Metal ions are required for *N*-deacetylase activity, but not for *N*-sulfotransferase activity.** *A*, comparison of *N*-sulfotransferase activity of NDST-1 with or without EDTA. The substrate employed for measuring *N*-sulfotransferase activity was *N*-deacetylated heparosan, and the reaction is shown at the *bottom* of the panel. *B*, effect of EDTA on *N*-deacetylase activity. The substrate employed for measuring *N*-deacetylase activity was heparosan, and the reactions are shown at the *bottom* of the panel. *Step 1*, NDST-1 was incubated with heparosan to allow the deacetylation reaction to occur. The reaction mixture was then heated at 100 °C to deactivate the enzyme. *Step 2*, recombinant *N*-sulfotransferase and [^{35}S]PAPS were then added to generate *N*-sulfation, where only those $GlcNH_2$ residues were susceptible to *N*-sulfotransferase modification. By measuring the amount of ^{35}S-labeled sulfated heparosan, we can determine the level of *N*-deacetylase activity. *C*, effects of different metal ions on *N*-deacetylase/*N*-sulfotransferase activity. The reaction involved in measuring the *N*-deacetylase/*N*-sulfotransferase activity is shown below. The data presented are the average value of three determinations, and the *error bars* indicate S.D.

that is a modification site for *N*-sulfotransferase activity as well as two GlcNAc residues (residues 1 and 5, Fig. 3*A*) that are modification sites for *N*-deacetylase or *N*-deacetylase/*N*-sulfotransferase activities. The 8-mer substrate exhibited greater than 95% purity as determined by high resolution anion-exchange chromatography (PAMN-HPLC) analysis (Fig. 3*A*).

To measure the reactivity to NDST-1 protein displaying *N*-deacetylase activity, the 8-mer substrate was incubated with the protein and Mn^{2+} but without the sulfo donor, PAPS. The lack of sulfo donor in the reaction abolished the *N*-sulfotransferase activity of the NDST-1 enzyme. A single product peak representing about 20% of the reaction mixture was detected by PAMN-HPLC, whereas 80% of the substrate remained unmodified (Fig. 3*B*). ESI-MS analysis confirmed the product to be deacetylated 8-mer, and the tandem MS analysis indicated that the deacetylation occurred at residue 5 (Fig. 4). The data suggest that *N*-deacetylase activity, although measurable, was minimal on the 8-mer substrate.

To measure the reactivity to NDST-1 protein displaying *N*-sulfotransferase activity, the 8-mer substrate was incubated with the protein and PAPS as well as EDTA, where the addition of EDTA was used to inhibit the deacetylase activity of NDST-1 enzyme. Under such condition, the 8-mer substrate was completely converted into 1NS 8-mer as determined by PAMN-HPLC (Fig. 3*C*). ESI-MS confirmed the product structure, and the tandem MS analysis located the *N*-sulfation site at residue 3 (data not shown). The data suggest that the 8-mer substrate displayed high reactivity to *N*-sulfotransferase activity without the participation of *N*-deacetylase.

To measure the reactivity to NDST-1 protein displaying both *N*-deacetylase and *N*-sulfotransferase activities, the 8-mer substrate was incubated with the protein and the sulfo donor, PAPS, in the presence of Mn^{2+} (Fig. 3*D*). Three products that differed by the number of GlcNS residues were obtained and resolved by PAMN-HPLC (Fig. 3*D*). No unmodified 8-mer substrate remained after the reaction, suggesting the substrate has high reactivity to the enzyme displaying both *N*-deacetylase and *N*-sulfotransferase activities. It should be noted that to obtain a mixture of products from the 8-mer substrate is consistent with a previous study (23).

Taken together, the data suggest that *N*-deacetylation is the limiting step during NDST-1-catalyzed conversion of a GlcNAc residue to a GlcNS residue. The rate of *N*-deacetylation is accelerated by combining with the *N*-sulfation reaction.

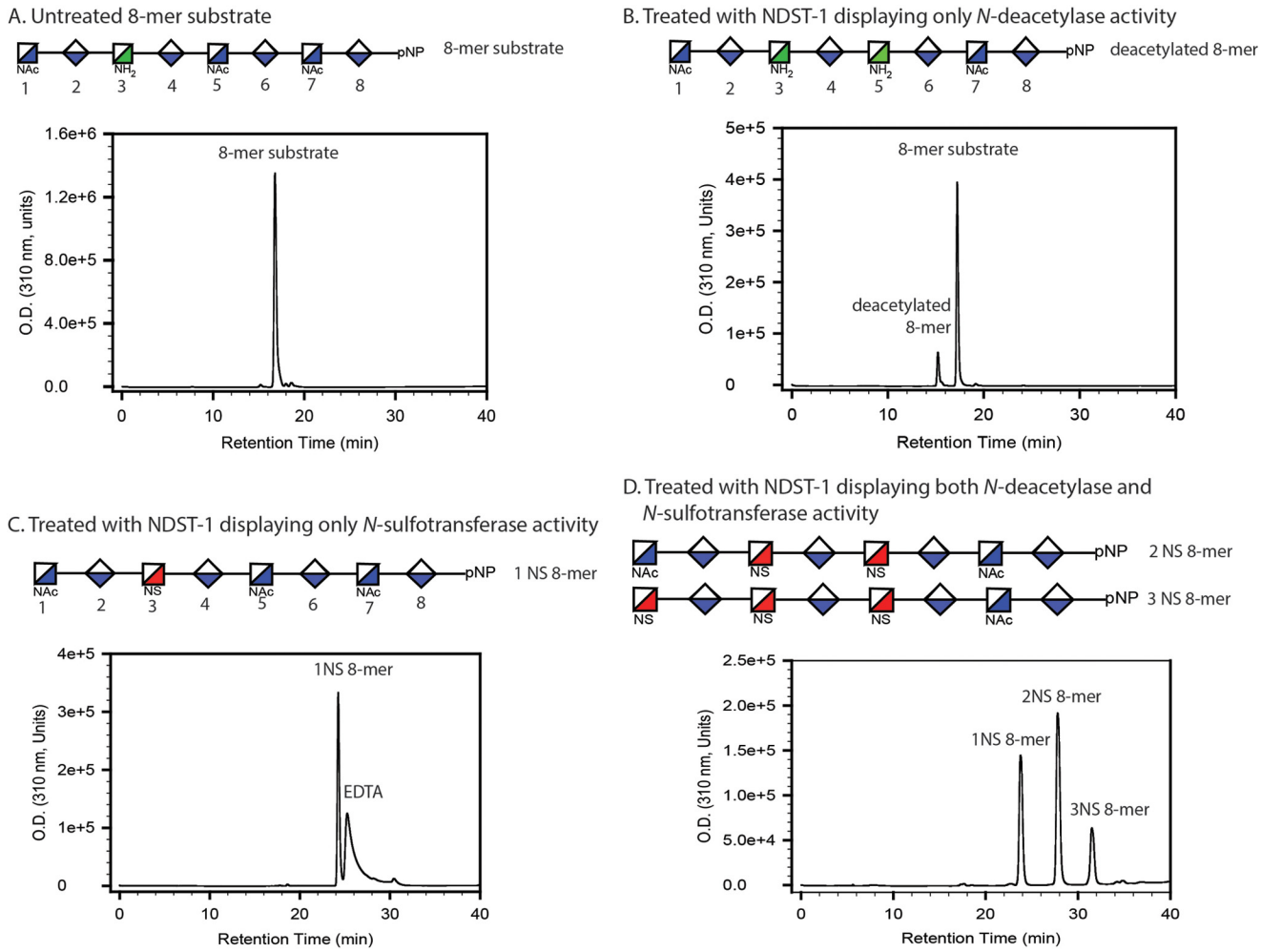

FIGURE 3. **Relative reactivity of *N*-deacetylase and *N*-sulfotransferase to a synthetic octasaccharide (8-mer) substrate.** *A*, PAMN-HPLC chromatogram of untreated 8-mer substrate. *B*, PAMN-HPLC chromatogram of the 8-mer substrate treated with NDST-1 (without PAPS) displaying only *N*-deacetylase activity. *C*, PAMN-HPLC chromatogram of the 8-mer substrate treated with NDST-1 (with EDTA) displaying only *N*-sulfotransferase activity. *D*, PAMN-HPLC chromatogram of the 8-mer substrate treated with NDST-1 (with PAPS) displaying both *N*-deacetylase and *N*-sulfotransferase activities. The schematic structures of the products from the modifications are shown in each panel. The structures of the products were confirmed by ESI-MS and tandem MS analysis.

Our data are consistent with previous findings using structurally heterogeneous polysaccharide substrates (32, 33).

Combination of N-Deacetylase and N-Sulfotransferase Activities Is Essential to Generate N-S Domains—NDST-1 is known for its capability to generate a domain that has consecutive repeating disaccharide units of -GlcA-GlcNS-, known as the N-S domain (23). Here, we examined whether both *N*-deacetylase and *N*-sulfotransferase on a single polypeptide are required to generate the N-S domain. To this end, the NDase (Arg^{66}–Phe^{604}) and NST (Leu^{557}–Arg^{882}) domains were expressed in insect cells using baculovirus expression (Fig. 1*C*). Using polysaccharide substrates, we found that NDase had comparable *N*-deacetylase activity to that of NDST-1 (Fig. 5*A*), and NST had comparable *N*-sulfotransferase to that of NDST-1 (Fig. 5*B*), suggesting that both individually expressed NDase and NST are active.

We next compared the ability to generate N-S domains from a mixture of NDase and NST proteins and the wild-type NDST-1 on a synthetic oligosaccharide substrate. To fully demonstrate the ability of the enzymes to form N-S domains, a long octadecasaccharide (18-mer, GlcNAc-(GlcA-GlcNAc)$_8$-GlcA-pNP) was synthesized, which has nine potential sites for enzymatic modifications. The purity of the 18-mer substrate was greater than 95% as determined by PAMN-HPLC (Fig. 6*A*). ESI-MS analysis of the 18-mer revealed its molecular weight to be 3553.6 ± 1, very close to the calculated the molecular weight (3553.0), confirming its structure (Fig. 6*B*).

Incubation of NDST-1 with the 18-mer substrate resulted in a mixture of 18-mer products that differed in the number of GlcNS residues, ranging from one to seven GlcNS residues (1NS 18-mer to 7NS 18-mer, Fig. 6*C*). The peaks labeled as 5NS 18-mer, 6NS 18-mer, and 7NS 18-mer were purified, and ESI-MS analyses were conducted to determine the molecular mass (Table 1). Tandem MS analysis confirmed the presence of N-S domains in the 18-mer products (data not shown). Additional products resulting from NDST-1-modified 18-mer substrate, including from 1NS 18-mer to 4NS 18-mer, were not analyzed by ESI-MS because each peak contained more than one component. Taken together, the results demonstrated that NDST-1 effectively modified the 18-mer substrate to generate the anticipated products. Modification of the 18-mer substrate with NDST-1 without PAPS only led to a minor amount of

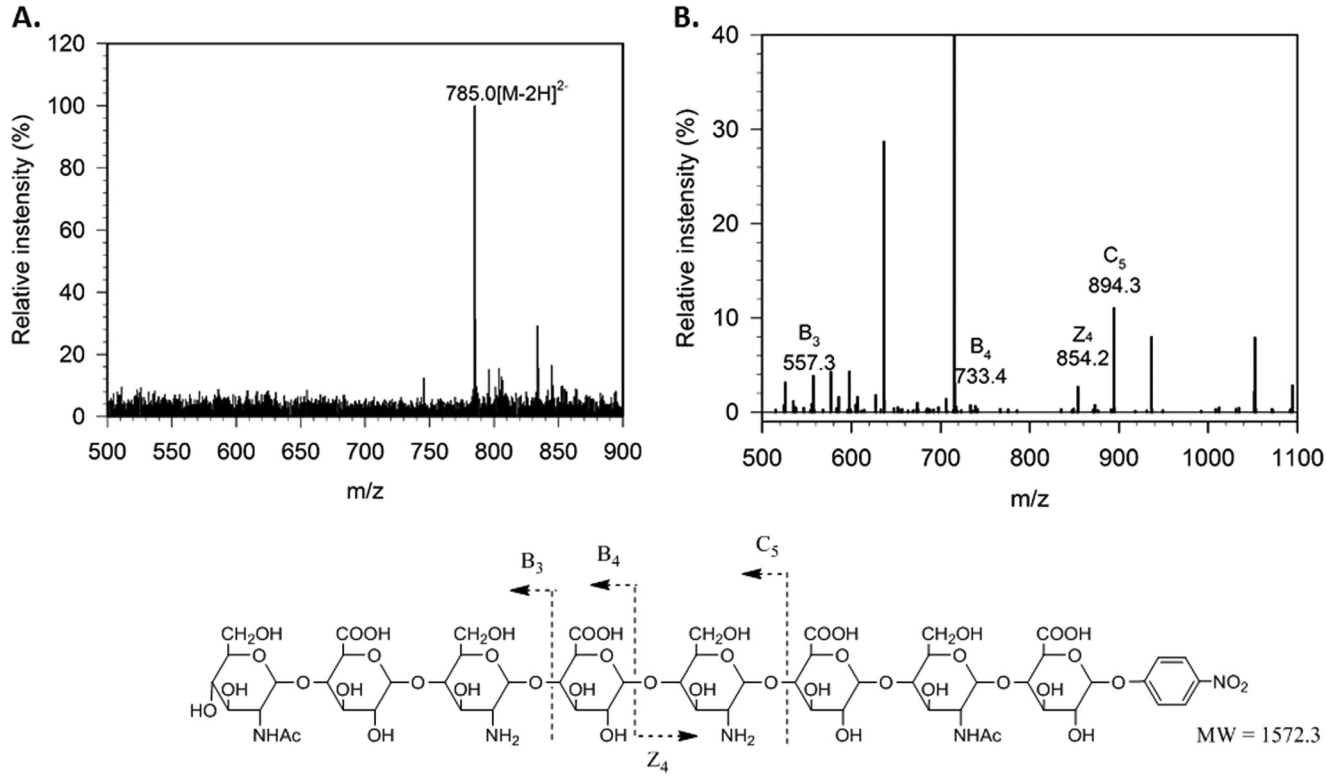

FIGURE 4. **MS analysis of deacetylated 8-mer.** The deacetylated 8-mer was first purified by HPLC prior to MS analysis. *A*, ESI-MS spectrum of deacetylated 8-mer. A molecular ion with the *m/z* value at 785.0 was detected, confirming that the molecular weight (*MW*) of the analyte to be 1572.0. The value is very close the calculated molecular weight of deacetylated 8-mer (1572.3). *B*, the tandem MS spectrum of deacetylated 8-mer. Precursor ion selection was at $[M-2H]^{2-}$, 785.0. The fragmentation pattern is depicted at the *bottom* of this figure.

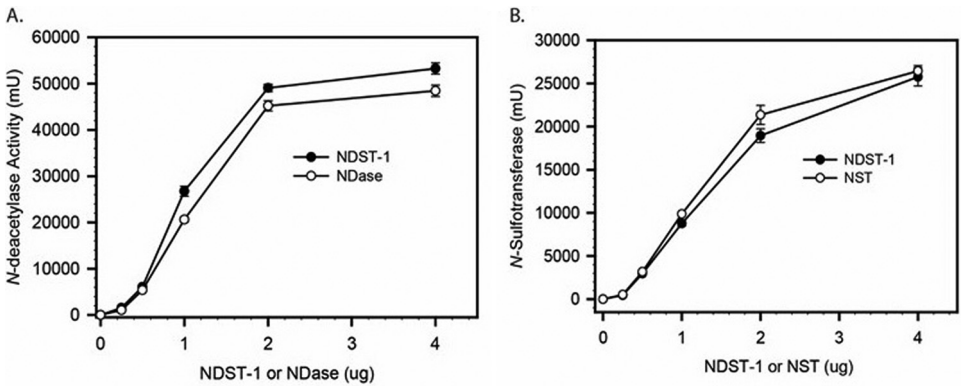

FIGURE 5. **Comparison of the *N*-deacetylase activity between NDST-1 and NDase as well as the *N*-sulfotransferase activity between NDST-1 and NST.** *A*, comparison of the *N*-deacetylase activity of purified NDST-1 and NDase. The measurement for the *N*-deacetylase activity, in the absence of PAPS, followed the procedures described at the *bottom* of Fig. 2*B* using heparosan as a substrate. *mU*, milliunits. *B*, comparison of *N*-sulfotransferase activity of purified NDST-1 and NST. The measurement for the *N*-sulfotransferase activity followed the procedures described at the *bottom* of Fig. 2*C* using deacetylated heparosan as a substrate. The data presented are the average value of three determinations, and the *error bars* indicate S.D.

deacetylated 18-mer product as in the case presented for the 8-mer substrate in Fig. 3*B*.

Starkly contrasting results were obtained from the 18-mer substrate modified by the mixture of two individually active NDase and NST proteins (Fig. 6*D*). Only a single 1NS product was obtained based on the HPLC analysis although sufficient amounts of NDase and NST proteins were included in the reaction, based on the activity measurement using polysaccharide substrates. Adding additional NDase enzyme into this reaction mixture did not significantly improve the efficiency to generate GlcNS residues, suggesting that two separate proteins displayed very low reactivity to the oligosaccharide substrate (data not shown). Our observation suggested that there is a cooperative effect to produce the N-S domain when both *N*-deacetylase and *N*-sulfotransferase activities are present on a single polypeptide. Disruption of the linkage between the *N*-deacetylase and *N*-sulfotransferase domains resulted in the inability to generate typical N-S sulfation patterns on the substrate.

To further support the apparent requirements for a bifunctional NDST-1 (not NDase and NST) in generating N-S domains, we compared the distributions of GlcNS residues in the ^{35}S-labeled polysaccharide products. In this experiment, heparosan (-(GlcNAc-GlcA)$_n$-) was incubated with either NDST-1 or a mixture of NDase and NST, in the presence of

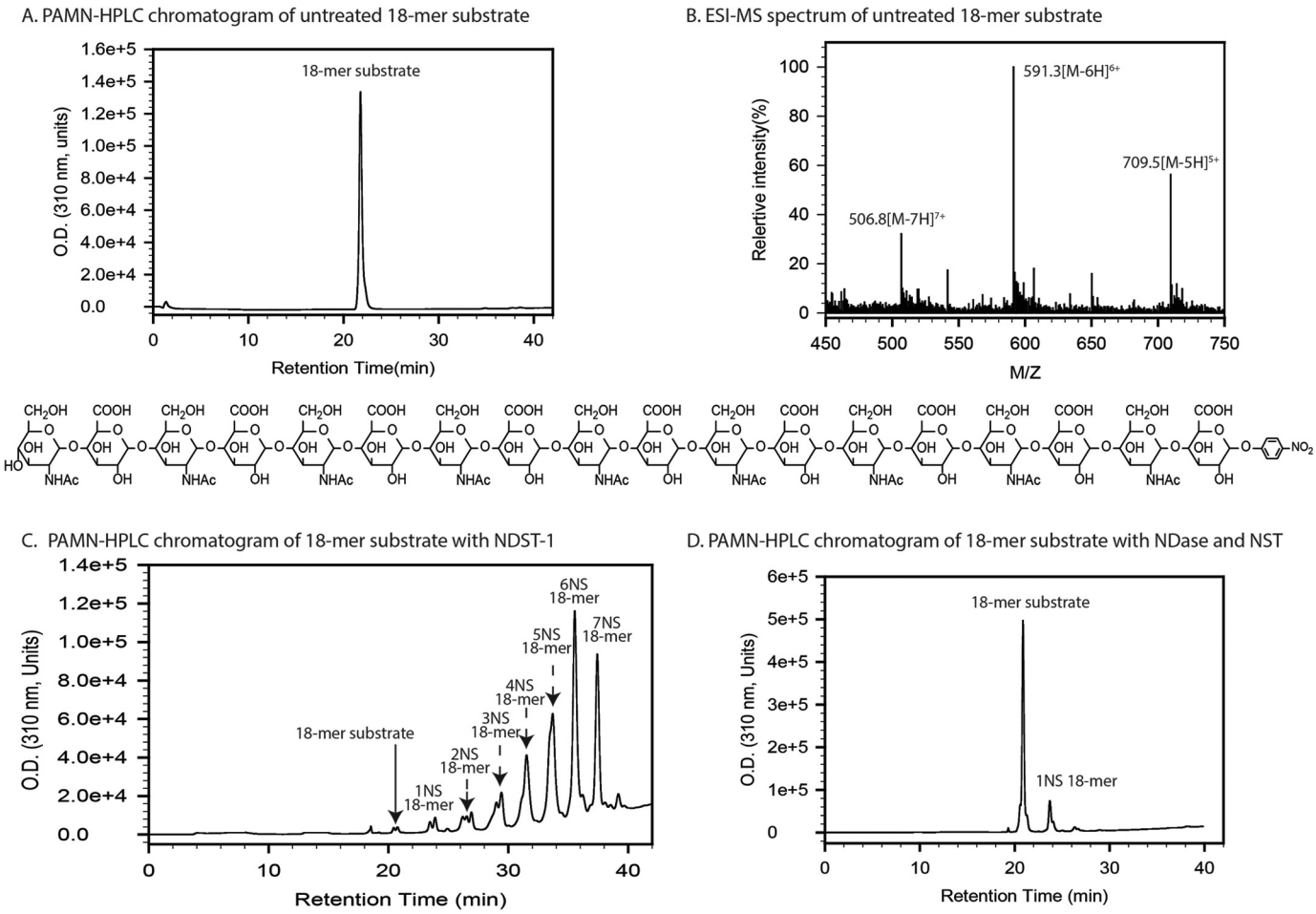

FIGURE 6. **Products of a mixture of NDase and NST *versus* NDST-1 on the 18-mer substrate.** *A*, PAMN-HPLC chromatogram of the 18-mer substrate. The compound was eluted as a single symmetric peak illustrating high substrate purity. *O. D.*, optical density. *B*, ESI-MS spectrum of the 18-mer substrate. The measured molecular weight was 3553.6 ± 1, very close to the calculated molecular weight (3553.0). *C*, PAMN-HPLC chromatogram of NDST-1-treated 18-mer substrate. A series of products ranging from the octadecasaccharide carrying one *N*-sulfo group to the octadecasaccharide carrying seven *N*-sulfo groups was present. The structures of 5NS 18-mer, 6NS 18-mer, and 7NS 18-mer were determined by ESI-MS as shown in Table 1. *D*, PAMN-HPLC chromatogram of the 18-mer substrate treated with a mixture of NDase and NST. Only a single 1NS 18-mer product was observed with the majority of the substrate unmodified.

TABLE 1

Results of MS analysis of NDST-1 modified 18-mer

MW, molecular weight.

	Abbreviated structures	Measured MW	Calculated MW
18-mer substrate	GlcNAc-GlcA-GlcNAc-GlcA-GlcNAc-GlcA-GlcNAc-GlcA-GlcNAc-GlcA-GlcNAc-GlcA-GlcNAc-GlcA-GlcNAc-GlcA-pNP	3553.6 ± 1.1	3553.0
5NS 18-mer product	GlcNAc-GlcA-GlcNAc-GlcA-GlcNAc-GlcA-GlcNS-GlcA-GlcNS-GlcA-GlcNS-GlcA-GlcNS-GlcA-GlcNS-GlcA-GlcNAc-GlcA-pNP	3743.5 ± 1.1	3743.1
6NS 18-mer product	GlcNAc-GlcA-GlcNAc-GlcA-GlcNS-GlcA-GlcNS-GlcA-GlcNS-GlcA-GlcNS-GlcA-GlcNS-GlcA-GlcNS-GlcA-GlcNAc-GlcA-pNP	3781.9 ± 1.1	3781.1
7NS 18-mer product	GlcNAc-GlcA-GlcNS-GlcA-GlcNS-GlcA-GlcNS-GlcA-GlcNS-GlcA-GlcNS-GlcA-GlcNS-GlcA-GlcNS-GlcA-GlcNAc-GlcA-pNP	3820.2 ± 2.0	3819.1

^{35}S-labeled PAPS, to generate to generate ^{35}S-labeled *N*-sulfated heparosan or *N*-[^{35}S]sulfo-heparosan. The resultant *N*-[^{35}S]sulfo-heparosan was depolymerized using nitrous acid as illustrated in the *bottom* of Fig. 7. Under these conditions, nitrous acid depolymerization cleaved -GlcNAc-GlcA- linkages, whereas the -GlcNS-GlcA- linkages remained intact (34). The depolymerized products were analyzed by gel permeation chromatography (Bio-Gel P-10) to resolve the oligosaccharides based on their sizes. As expected, *N*-[^{35}S]sulfo-heparosan prepared by NDST-1 showed a ladder of ^{35}S-labeled oligosaccharides from tetrasaccharide to >decasaccharides, which contained -GlcNS-GlcA- repeating units (Fig. 7*A*). These data demonstrated that N-S domains were present in the *N*-[^{35}S]sulfo-heparosan prepared by NDST-1. In contrast, only ^{35}S-labeled tetrasaccharide was obtained from the depolymerized *N*-[^{35}S]sulfo-heparosan prepared by a mixture of NDase and NST (Fig. 7*B*). These data demonstrated that the GlcNS residues in the polysaccharide product occurred in isolation, not in the form of N-S domains. Taken together, our data from the analysis of GlcNS residue distribution in the polysaccharide

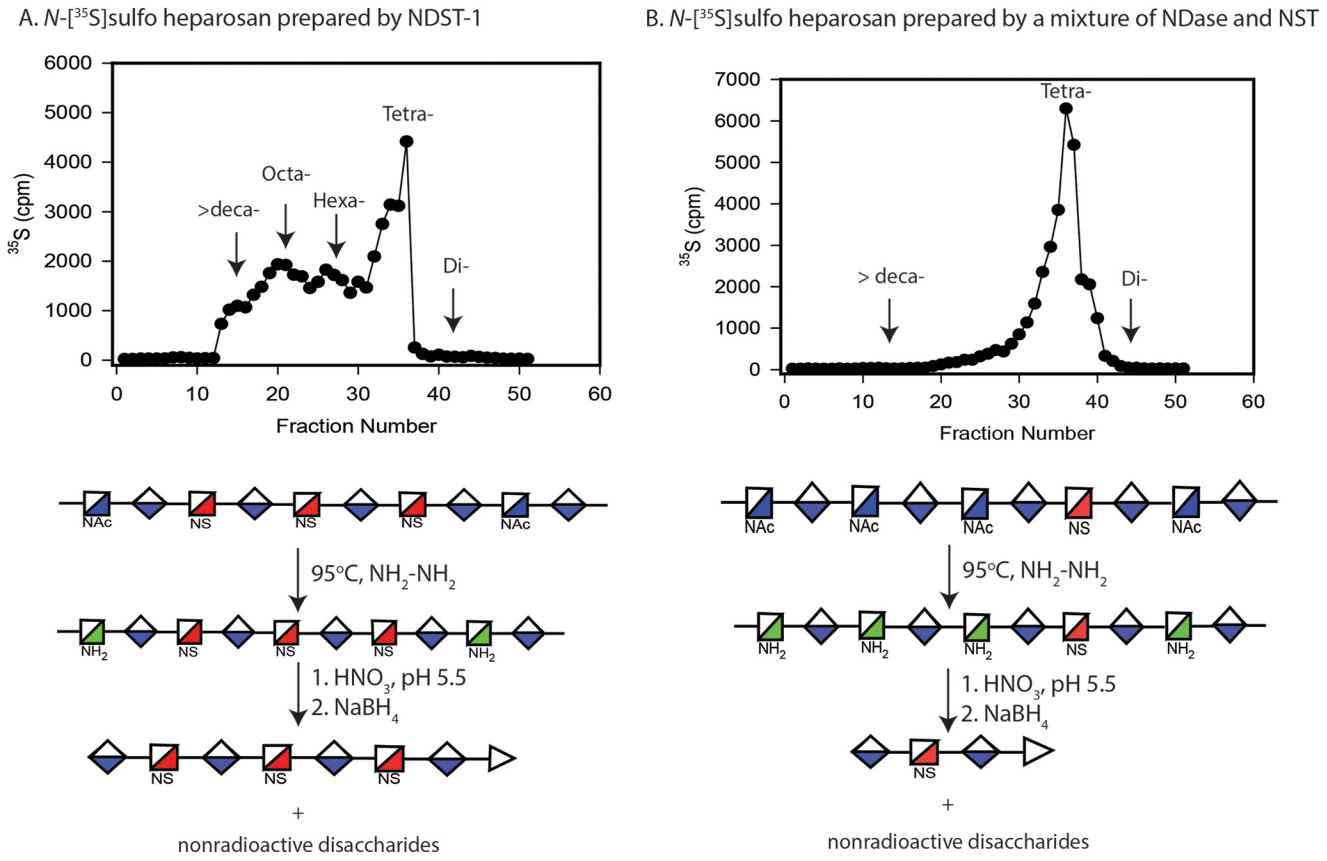

FIGURE 7. **Determination of the distribution of GlcNS residues in the *N*-[^{35}S]sulfo-heparosan prepared by NDST-1 and the mixture of NDase and NST.** *A*, Bio-Gel P-10 elution profile of nitrous acid-degraded *N*-[^{35}S]sulfo-heparosan prepared by NDST-1. *B*, Bio-Gel P-10 elution profile of nitrous acid-degraded *N*-[^{35}S]sulfo-heparosan prepared by the mixture of the individual expressed NDase and NST proteins. The reactions involved in chemical deacetylation and nitrous acid depolymerization are shown below each profile. The products also contained nonradioactive disaccharides, which were not visible under the experimental conditions. The elution positions of different sized oligosaccharides are indicated in *panels A* and *B*.

TABLE 2

Reactivity of HS sulfotransferases to two *N*-sulfated heparosan constructs

Enzymes	*N*-Sulfated heparosan made by NDST-1[a]	*N*-Sulfated heparosan made by a mixture of NDase and NST[b]
	cpm	
Control, no enzymes	131	165
2-OST/C5-epi[c]	24,336	2013
6-OST[d]	1843	2489

[a] Heparosan (50 μg) was incubated with NDST-1 (4 μg) and 100 μM PAPS in 1 ml of reaction buffer overnight. The product was purified by a DEAE column, dialyzed to remove NaCl, and dried. The sample was then reconstituted in 50 μl of water.

[b] Heparosan (50 μg) was incubated with NDase (4 μg) and NST (2 μg) and 100 μM PAPS in 1 ml of reaction buffer overnight. The product was purified by a DEAE column, dialyzed to remove NaCl, and dried. The sample was then reconstituted in 50 μl of water.

[c] Both 2-OST (0.2 μg) and C5-epi (0.2 μg) were incubated with 5 μg of *N*-sulfated heparosan and 1×10^5 cpm [^{35}S]PAPS and 1 μM unlabeled PAPS at 37 °C for 1 h. The product was loaded onto a DEAE column to determine the amount of ^{35}S-labeled product.

[d] 6-OST-1 (0.2 μg) was incubated with 5 μg of *N*-sulfated heparosan and 1×10^5 cpm [^{35}S]PAPS and 1 μM unlabeled PAPS at 37 °C for 1h. The product was loaded onto a DEAE column to determine the amount of ^{35}S-labeled product.

products are consistent with those obtained using the structurally defined 18-mer substrate.

We then compared the susceptibility of two differently *N*-sulfated heparosans to modification of other HS biosynthetic enzymes, such as C_5-epi and 2-OST (Table 2). One type of *N*-sulfated heparosan was prepared by wild-type NDST-1, and another was prepared by the mixture of NDase and NST. Indeed, the *N*-sulfated heparosan prepared by the mixture of two enzymes showed about 13-fold lower reactivity toward epimerase and 2-OST than the one synthesized by full-length NDST-1. In a control experiment, the two compounds exhibited comparable reactivity to 6-OST-1 modification consistent with this modification not being influenced by the level of *N*-sulfation (35–37). The data suggest that change in the N-S domain structures impacts the biosynthesis of HS.

Discussion

As the first modification enzyme in the HS biosynthetic pathway, NDST-1 plays a critical role in producing the GlcNS residues that direct subsequent enzymatic modifications to form HS with elaborate sulfation patterns (38). Here, utilizing highly purified recombinant enzymes and structurally defined oligosaccharide substrates, we investigated the interplay between *N*-deacetylase and *N*-sulfotransferase activity of NDST-1 and their roles in forming N-S domains. The crucial innovation in our work is the access to recombinant forms of *N*-deacetylase and *N*-sulfotransferase as well as full-length NDST-1 proteins and the use of structurally defined oligosaccharide substrates. Our data suggest that the activity of *N*-deacetylase can be greatly enhanced by the presence of *N*-sulfotransferase activity, but such enhancement is only obtained when both activities are present in a single polypeptide. When physically separated, the two independent *N*-deacetylase and *N*-sulfotransferase

domains do not display the same sulfation patterns as that of the intact NDST-1 protein, diminishing the ability to form HS with desired biological functions. In fact, the bifunctionality of NDST is highly conserved in all organisms that generate HS, supporting the necessity for linking these separate activities to generate N-S domains. The modification mechanism catalyzed by NDST-1 is a complex system involving two enzymatic activities and is influenced by both the macromolecular substrate and the PAPS cofactor. Understanding of the cooperative mechanism will be greatly enhanced by structural information of the full-length NDST-1.

Our data suggest that *N*-deacetylase activity is the limiting step in the process of converting a GlcNAc residue to a GlcNS residue. This is also supported by the fact that NST expressed in *E. coli* is highly active on a polysaccharide substrate with -$(GlcNH_2\text{-}GlcA)_n$- repeating units (39). The *N*-deacetylase activity can be regulated by the presence of metal ions. Histone deacetylase, an enzyme that removes the acetyl group from acetylated lysine residues, requires a zinc ion for catalysis (40). Unlike histone deacetylase, *N*-deacetylase activity from NDST-1 is not mediated by zinc ions. This difference is perhaps not surprising given that these enzymes follow very different reaction mechanisms. In the case of the histone deacetylase, the acetyl group from a lysine residue is transferred to CoA to form acetyl-CoA (41), whereas there is no CoA cofactor involvement in the NDST-catalyzed reactions. Like NDST-1, other deacetylases such as peptidoglycan deacetylase from *Streptococcus pneumoniae* and acetylxylan esterases from *Streptomyces lividans* and *Clostridium thermocellum* reportedly do not require co-factors but do utilize divalent ions such as Zn^{2+} or Co^{2+} for catalysis (42, 43). The activity of NDST-1 that was depleted with metal ions via dialysis can be rescued by the addition of Ca^{2+}, Mn^{2+}, Co^{2+}, or Mg^{2+}, suggesting that removal of metal ions from the protein does not cause irreversible structural changes. At the present time, we do not know whether a divalent ion also participates in direct binding to the saccharide substrate.

Although there is no clear evidence to link the concentration of divalent ions to the biosynthesis of HS *in vivo*, the potential impact of PAPS concentration on the N-S domain formation has been documented (44). Sasaki *et al.* reported that mutation or inhibition of PAPS transporter, a protein that transports PAPS into the Golgi apparatus to carry out HS biosynthesis, reduced the self-renewal and proliferation of mouse embryonic stem cells. The authors attributed these effects to the change in the activities of NDSTs, including NDST-1 and NDST-2 (44). The concentration of PAPS has been known to play a role in controlling the activity of NDST-1 using a structurally heterogeneous polysaccharide substrate in an *in vitro* experiment (45). Carlsson *et al.* (45) concluded that NDST only displayed "random and limited *N*-deacetylation" in the absence of PAPS, consistent with our observation. In our study, structurally defined oligosaccharide substrates and highly purified recombinant NDase, NST, and NDST-1 were utilized, allowing us to confirm their conclusion and demonstrate the necessity of the deacetylase to be coupled to the sulfotransferase as a bifunctional enzyme.

Previously, it has been suggested that the length of the N-S domains may be controlled by the presence of different isoforms of NDST (11, 46). For example, HS from mast cells where NDST-2 is the dominant isoform has much larger N-S domains. Another possible mechanism for regulating the length of N-S domains may be by controlling the cellular concentration of PAPS. At higher concentrations of PAPS, longer N-S domains may be formed because such conditions enhance the activity of NDST-1, whereas shorter N-S domains may be formed if the cellular concentration of PAPS is lower due to a slower reaction rate of NDST-1. Continuing efforts toward understanding the cooperative nature of the *N*-deacetylase and *N*-sulfotransferase activities of NDST-1 and other NDST isoforms will help reveal the regulatory mechanisms of HS biosynthesis.

Author Contributions—W. D. expressed the enzymes and characterized the substrate specificity. Y. X. synthesized oligosaccharide substrates. V. P. prepared expression constructs. L. C. P. designed the experiment. J. L. designed the experiment and wrote the manuscript.

Acknowledgments—We thank Dr. K. Moremen (University of Georgia) for insightful discussion and A. F. Moon and Dr. G. A. Mueller (NIEHS, National Institutes of Health) for critical reading of the manuscript.

References

1. Bishop, J. R., Schuksz, M., and Esko, J. D. (2007) Heparan sulphate proteoglycans fine-tune mammalian physiology. *Nature* **446,** 1030–1037
2. Gama, C. I., Tully, S. E., Sotogaku, N., Clark, P. M., Rawat, M., Vaidehi, N., Goddard, W. A., 3rd, Nishi, A., and Hsieh-Wilson, L. C. (2006) Sulfation patterns of glycosaminoglycans encode molecular recognition and activity. *Nat. Chem. Biol.* **2,** 467–473
3. Liu, J., and Linhardt, R. J. (2014) Chemoenzymatic synthesis of heparan sulfate and heparin. *Nat. Prod. Rep.* **31,** 1676–1685
4. Xu, Y., Masuko, S., Takieddin, M., Xu, H., Liu, R., Jing, J., Mousa, S. A., Linhardt, R. J., and Liu, J. (2011) Chemoenzymatic synthesis of homogeneous ultra-low molecular weight heparin. *Science* **334,** 498–501
5. Xu, Y., Cai, C., Chandarajoti, K., Hsieh, P. H., Li, L., Pham, T. Q., Sparkenbaugh, E. M., Sheng, J., Key, N. S., Pawlinski, R., Harris, E. N., Linhardt, R. J., and Liu, J. (2014) Homogeneous and reversible low-molecular weight heparins with reversible anticoagulant activity. *Nat. Chem. Biol.* **10,** 248–250
6. Li, J.-P., Gong, F., El Darwish, K., Jalkanen, M., and Lindahl, U. (2001) Characterization of the D-glucuronyl C5-epimerase involved in the biosynthesis of heparin and heparan sulfate. *J. Biol. Chem.* **276,** 20069–20077
7. Sheng, J., Xu, Y., Dulaney, S. B., Huang, X., and Liu, J. (2012) Uncovering biphasic catalytic mode of C5-epimerase in heparan sulfate biosynthesis. *J. Biol. Chem.* **287,** 20996–21002
8. Rong, J., Habuchi, H., Kimata, K., Lindahl, U., and Kusche-Gullberg, M. (2001) Substrate specificity of the heparan sulfate hexuronic acid 2-*O*-sulfotransferase. *Biochemistry* **40,** 5548–5555
9. Liu, C., Sheng, J., Krahn, J. M., Perera, L., Xu, Y., Hsieh, P. H., Dou, W., Liu, J., and Pedersen, L. C. (2014) Molecular mechanism of substrate specificity for heparan sulfate 2-*O*-sulfotransferase. *J. Biol. Chem.* **289,** 13407–13418
10. Xu, D., Moon, A. F., Song, D., Pedersen, L. C., and Liu, J. (2008) Engineering sulfotransferases to modify heparan sulfate. *Nat. Chem. Biol.* **4,** 200–202
11. Aikawa, J., and Esko, J. D. (1999) Molecular cloning and expression of a third member of the heparan sulfate/heparin GlcNAc *N*-deacetylase/*N*-sulfotransferase family. *J. Biol. Chem.* **274,** 2690–2695
12. Aikawa, J.-i., Grobe, K., Tsujimoto, M., and Esko, J. D. (2001) Multiple isozymes of heparan sulfates/heparin GlcNAc *N*-deacetylase/GlcN *N*-sul-

fotransferase: Structure and activity of the fourth member, NDST4. *J. Biol. Chem.* **276,** 5876–5882
13. Fan, G., Xiao, L., Cheng, L., Wang, X., Sun, B., and Hu, G. (2000) Targeted disruption of NDST-1 gene leads to pulmonary hypoplasia and neonatal respiratory distress in mice. *FEBS Lett.* **467,** 7–11
14. MacArthur, J. M., Bishop, J. R., Stanford, K. I., Wang, L., Bensadoun, A., Witztum, J. L., and Esko, J. D. (2007) Liver heparan sulfate proteoglycans mediate clearance of triglyceride-rich lipoproteins independently of LDL receptor family members. *J. Clin. Invest.* **117,** 153–164
15. Crawford, B. E., Garner, O. B., Bishop, J. R., Zhang, D. Y., Bush, K. T., Nigam, S. K., and Esko, J. D. (2010) Loss of the heparan sulfate sulfotransferase, *Ndst1*, in mammary epithelial cells selectively blocks lobuloalveolar development in mice. *PLoS One* **5,** e10691
16. Wang, L., Fuster, M., Sriramarao, P., and Esko, J. D. (2005) Endothelial heparan sulfate deficiency impairs L-selectin- and chemokine-mediated neutrophil trafficking during inflammatoray responses. *Nat. Immunol.* **6,** 902–910
17. Fuster, M. M., Wang, L., Castagnola, J., Sikora, L., Reddi, K., Lee, P. H. A., Radek, K. A., Schuksz, M., Bishop, J. R., Gallo, R. L., Sriramarao, P., and Esko, J. D. (2007) Genetic alteration of endothelial heparan sulfate selectively inhibits tumor angiogenesis. *J. Cell Biol.* **177,** 539–549
18. Reuter, M. S., Musante, L., Hu, H., Diederich, S., Sticht, H., Ekici, A. B., Uebe, S., Wienker, T. F., Bartsch, O., Zechner, U., Oppitz, C., Keleman, K., Jamra, R. A., Najmabadi, H., Schweiger, S., Reis, A., and Kahrizi, K. (2014) *NDST1* missense mutations in autosomal recessive intellectual disability. *Am. J. Med. Genet. Part A* **164A,** 2753–2763, 10.1002/ajmg.a.36723
19. Forsberg, E., Pejler, G., Ringvall, M., Lunderius, C., Tomasini-Johansson, B., Kusche-Gullberg, M., Eriksson, I., Ledin, J., Hellman, L., and Kjellén, L. (1999) Abnormal mast cells in mice deficient in a heparin-synthesizing enzyme. *Nature* **400,** 773–776
20. Pallerla, S. R., Lawrence, R., Lewejohann, L., Pan, Y., Fischer, T., Schlomann, U., Zhang, X., Esko, J. D., and Grobe, K. (2008) Altered heparan sulfate structure in mice with deleted *NDST3* gene function. *J. Biol. Chem.* **283,** 16885–16894
21. Murphy, K. J., Merry, C. L. R., Lyon, M., Thompson, J. E., Roberts, I. S., and Gallagher, J. T. (2004) A new model for the domain structure of heparan sulfate based on the novel specificity of K5 lyase. *J. Biol. Chem.* **279,** 27239–27245
22. Kreuger, J., Spillmann, D., Li, J.-p., and Lindahl, U. (2006) Interactions between heparan sulfate and proteins: the concept of specificity. *J. Cell Biol.* **174,** 323–327
23. Sheng, J., Liu, R., Xu, Y., and Liu, J. (2011) The dominating role of *N*-deacetylase/*N*-sulfotransferase 1 in forming domain structures in heparan sulfate. *J. Biol. Chem.* **286,** 19768–19776
24. Liu, J., Shriver, Z., Blaiklock, P., Yoshida, K., Sasisekharan, R., and Rosenberg, R. D. (1999) Heparan sulfate D-glucosaminyl 3-*O*-sulfotransferase-3A sulfates *N*-unsubstituted glucosamine residues. *J. Biol. Chem.* **274,** 38155–38162
25. Kakuta, Y., Sueyoshi, T., Negishi, M., and Pedersen, L. C. (1999) Crystal structure of the sulfotransferase domain of human heparan sulfate *N*-deacetylase/*N*-sulfotransferase 1. *J. Biol. Chem.* **274,** 10673–10676
26. Chen, J., Jones, C. L., and Liu, J. (2007) Using an enzymatic combinatorial approach to identify anticoagulant heparan sulfate structures. *Chem. Biol.* **14,** 986–993
27. Peterson, S., and Liu, J. (2012) Deciphering mode of action heparanase using structurally defined oligosaccharides. *J. Biol. Chem.* **287,** 34836–34843
28. Shively, J. E., and Conrad, H. E. (1976) Formation of anhydrosugars in the chemical depolymerization of heparin. *Biochemistry* **15,** 3932–3942
29. Saribaş, A. S., Mobasseri, A., Pristatsky, P., Chen, X., Barthelson, R., Hakes, D., and Wang, J. (2004) Production of *N*-sulfated polysaccharides using yeast expressed *N*-deacetylase/*N*-sulfotransferase-1 (NDST-1). *Glycobiology* **14,** 1217–1228
30. Duncan, M. B., Liu, M., Fox, C., and Liu, J. (2006) Characterization of the *N*-deacetylase domain from the heparan sulfate *N*-deacetylase/*N*-sulfotransferase 2. *Biochem. Biophys. Res. Commun.* **339,** 1232–1237
31. Riesenfeld, J., Höök, M., and Lindahl, U. (1980) Biosynthesis of heparin: assay and properties of the microsomal *N*-acetyl-D-glucosaminyl *N*-deacetylase. *J. Biol. Chem.* **255,** 922–928
32. Riesenfeld, J., Höök, M., and Lindahl, U. (1982) Biosynthesis of heparan sulfate in rat liver. *J. Biol. Chem.* **257,** 7050–7055
33. Bengtsson, J., Eriksson, I., and Kjellén, L. (2003) Distinct effects on heparan sulfate structure by different active site mutations in NDST-1. *Biochemistry* **42,** 2110–2115
34. Shaklee, P. N., and Conrad, H. E. (1984) Hydrazinolysis of heparin and other glycosaminoglycans. *Biochem. J.* **217,** 187–197
35. Liu, R., and Liu, J. (2011) Enzymatical placement of 6-*O*-sulfo groups in heparan sulfate. *Biochemistry* **50,** 4382–4391
36. Smeds, E., Habuchi, H., Do, A.-T., Hjertson, E., Grundberg, H., Kimata, K., Lindahl, U., and Kusche-Gullberg, M. (2003) Substrate specificities of mouse heparan sulphate glucosaminyl 6-*O*-sulfotransferases. *Biochem. J.* **372,** 371–380
37. Jemth, P., Smeds, E., Do, A.-T., Habuchi, H., Kimata, K., Lindahl, U., and Kusche-Gullberg, M. (2003) Oligosaccharide library-based assessment of heparan sulfate 6-*O*-sulfotransfer substrate specificity. *J. Biol. Chem.* **278,** 24371–24376
38. Esko, J. D., and Selleck, S. B. (2002) Order out of chaos: Assembly of ligand binding sites in heparan sulfate. *Annu. Rev. Biochem.* **71,** 435–471
39. Liu, R., Xu, Y., Chen, M., Weïwer, M., Zhou, X., Bridges, A. S., DeAngelis, P. L., Zhang, Q., Linhardt, R. J., and Liu, J. (2010) Chemoenzymatic design of heparan sulfate oligosaccharides. *J. Biol. Chem.* **285,** 34240–34249
40. Miller, T. A., Witter, D. J., and Belvedere, S. (2003) Histone acetylase inhibitors. *J. Med. Chem.* **46,** 5097–5116
41. Mottet, D., and Castronovo, V. (2008) Histone deacetylases: target enzymes for cancer therapy. *Clin. Exp. Metastasis* **25,** 183–189
42. Blair, D. E., Schüttelkopf, A. W., MacRae, J. I., and van Aalten, D. M. F. (2005) Structure and metal-dependent mechanism of peptidoglycan deacetylase, a streptococcal virulent factor. *Proc. Natl. Acad. Sci. U.S.A.* **102,** 15429–15434
43. Taylor, E. J., Gloster, T. M., Turkenburg, J. P., Vincent, F., Brzozowski, A. M., Dupont, C., Shareck, F., Centeno, M. S., Prates, J. A., Puchart, V., Ferreira, L. M., Fontes, C. M. G. A., Biely, P., and Davies, G. J. (2006) Structure and activity of two metal ion-dependent acetylxylan esterase involved in plant cell wall degradation reveals a close similarity to peptidoglycan deacetylases. *J. Biol. Chem.* **281,** 10968–10975
44. Sasaki, N., Hirano, T., Ichimiya, T., Wakao, M., Hirano, K., Kinoshita-Toyoda, A., Toyoda, H., Suda, Y., and Nishihara, S. (2009) The 3′-phosphoadenosine 5′-phosphosulfate transporters, PAPST1 and 2, contribute to the maintenance and differentiation of mouse embryonic stem cells. *PLoS One* **4,** e8262
45. Carlsson, P., Presto, J., Spillmann, D., Lindahl, U., and Kjellén, L. (2008) Heparin/heparan sulfate biosynthesis Processive formation of *N*-sulfated domains. *J. Biol. Chem.* **283,** 20008–20014
46. Kusche-Gullberg, M., Eriksson, I., Pikas, D. S., and Kjellén, L. (1998) Identification and expression in mouse of two heparan sulfate glucosaminyl *N*-deacetylase/*N*-sulfotransferase genes. *J. Biol. Chem.* **273,** 11902–11907